

## **Stimulation of surface IgM of chronic lymphocytic leukemia cells induces an unfolded protein response dependent on BTK and SYK**

Sergey Krysov<sup>1,\*</sup>, Andrew J Steele<sup>1</sup>, Vania Coelho<sup>1</sup>, Adam Linley<sup>1</sup>, Marina Sanchez Hidalgo<sup>1</sup>, Matthew Carter<sup>1</sup>, Kathleen N Potter<sup>1</sup>, Benjamin Kennedy<sup>2</sup>, Andrew S Duncombe<sup>3</sup>, Margaret Ashton-Key<sup>1,4</sup>, Francesco Forconi<sup>1,3</sup>, Freda K Stevenson<sup>1</sup>, Graham Packham<sup>1</sup>

<sup>1</sup>Cancer Research UK Centre, Cancer Sciences Unit, University of Southampton Faculty of Medicine, Southampton General Hospital, Southampton, SO16 6YD, UK

<sup>2</sup>Medical Research Council Toxicology Unit, University of Leicester, Leicester, UK

<sup>3</sup>Department of Haematology, University Hospital Southampton, Southampton, SO16 6YD, UK

<sup>4</sup>Department of Cellular Pathology, University Hospital Southampton, Southampton General Hospital, Southampton, UK

\*corresponding author. Dr Sergey Krysov. Barts Cancer Institute, Queen Mary, University of London, John Vane Science Centre, Charterhouse Square, London, EC1M 6BQ, UK. Tel. [44] (0)20 7882 3816. Fax. [44] (0)20 7882 3891. Email: s.krysov@qmul.ac.uk

Current addresses.

SK. Barts Cancer Institute, Queen Mary, University of London, John Vane Science Centre, Charterhouse Square, London, EC1M 6BQ, UK

VC. Hematology Department, University College of London – Cancer Institute, 72 Huntley Street, London, WC1E 6BT, UK

MSH. Department of Pharmacology, University of Seville, No. 2 41012, Seville, Spain

Word count; 4242

Abstract count; 200

Figures; 7

Tables; 0

## **Key points;**

1. Stimulation of the B-cell receptor of chronic lymphocytic leukemia cells results in activation of an unfolded protein response.
2. Unfolded protein response activation following surface immunoglobulin M stimulation *in vitro* is dependent on the activity of BTK and SYK.

## **Abstract**

B-cell receptor (BCR) signaling plays a key role in the behavior of chronic lymphocytic leukemia (CLL). However, cellular consequences of signaling are incompletely defined. Here we explored possible links between BCR signaling and the unfolded protein response (UPR), a stress response pathway which can promote survival of normal and malignant cells. Compared to normal B cells, circulating CLL cells expressed increased, but variable, levels of UPR components. Higher expression of *CHOP* and *XBP1* RNAs were associated with more aggressive disease. UPR activation appeared due to prior tissue-based antigenic stimulation since elevated expression of UPR components was detected within lymph node proliferation centers. Basal UPR activation also correlated closely with surface IgM (sIgM) signaling capacity *in vitro* in both *IGHV* unmutated (U)CLL and within mutated (M)CLL. sIgM signaling increased UPR activation *in vitro* with responders showing increased expression of *CHOP* and *XBP1* RNAs, and PERK and BIP proteins, but not *XBP1* splicing. Inhibitors of BCR-associated kinases effectively prevented sIgM-induced UPR activation. Overall, the study demonstrates that sIgM signaling results in activation of some components the UPR in CLL cells. Modulation of the UPR may contribute to variable clinical behavior, and its inhibition may contribute to clinical responses to BCR-associated kinase inhibitors.

**Key words;** chronic lymphocytic leukemia; unfolded protein response; B-cell receptor; kinase inhibitor; outcome; ibrutinib; BTK; SYK.

## Introduction

Chronic lymphocytic leukemia (CLL) provides a unique opportunity to understand how antigen can influence the behavior of malignant lymphocytes. It also acts as a model for the development of novel therapies targeted towards B-cell receptor (BCR) signaling pathways.<sup>1-4</sup> CLL comprises two major subsets with differing levels of somatic hypermutation of tumor *IGV* genes. CLL with unmutated *IGV* (U-CLL) derives from naïve CD5<sup>+</sup>CD27<sup>-</sup> B cells of the normal natural antibody repertoire, whereas CLL with mutated *IGV* genes (M-CLL) may derive from post-germinal center CD5<sup>+</sup>CD27<sup>+</sup> cells.<sup>5,6</sup> Importantly, these subsets have distinct clinical behavior and U-CLL has a more aggressive clinical course. Antigen signaling is thought to be on-going in both subsets and, rather than the presence or absence of signaling, it is the balance between distinct types of responses that appears to determine clinical behavior.<sup>1</sup> Anergy, a state of cellular lethargy that is induced following antigen engagement in the absence of T-cell help,<sup>7</sup> is observed in all CLL but is particularly prominent in M-CLL.<sup>1</sup> By contrast, positive antigen signaling leading to proliferation and survival appears more evident in U-CLL. The importance of antigen signaling for CLL is emphasized by recent results which have demonstrated the clinical effectiveness of inhibitors of BCR-associated kinases.<sup>8</sup>

Antigen engagement *in vivo* is thought to occur within proliferation centers (PC) found predominantly in the lymph nodes (LN) of CLL patients. Following stimulation, CLL cells enter the circulation and therefore carry a temporary “imprint” of their prior tissue based stimulation.<sup>9,10</sup> Thus, markers of anergy,<sup>7</sup> including strong down-modulation of surface IgM (sIgM) expression and signaling capacity, raised ERK1/2 phosphorylation and NFAT expression, can be detected in blood CLL cells, most prominently in M-CLL.<sup>11-13</sup> In contrast to M-CLL, blood cells from patients with U-CLL tend to retain sIgM expression and signaling responsiveness, and express higher levels of markers of “positive” BCR signaling, including the proliferation and survival-promoting proteins, MYC and MCL1.<sup>14,15</sup> Positive signaling can be mimicked *in vitro* by treating CLL cells with anti-IgM antibodies which increases expression of these markers in samples that retain sIgM responsiveness.<sup>16,17</sup> Although the overall behavior of U-CLL and M-CLL is distinct, there is heterogeneity within these subsets, especially within M-CLL.<sup>11</sup> For example, high levels of sIgM expression and signaling in M-CLL may highlight a subset at higher risk of progression. Indeed, our previous study demonstrated that anti-IgM-induced BIM phosphorylation was associated with requirement for treatment, including within the M-CLL subset.<sup>18</sup>

Despite recent advances, the consequences of BCR stimulation in CLL remain incompletely understood. In this work we have investigated the effects of sIgM stimulation on the unfolded protein response (UPR). The UPR has been most widely studied as a stress response pathway which responds to accumulation of unfolded/mis-folded proteins and/or elevated secretory protein synthesis within

the endoplasmic reticulum (ER) lumen.<sup>19,20</sup> See **Supplementary Figure 1** for a summary of UPR molecules and pathways.

In B cells, the UPR plays key roles in differentiation since production of secreted immunoglobulin (Ig) by plasma cells requires a compensatory increase in protein production capacity mediated by UPR induction.<sup>21</sup> Thus, XBP1 and IRE1 are essential for plasma cell development.<sup>22-24</sup> The UPR is also essential for the survival of multiple myeloma cells and is an established therapeutic target in this disease.<sup>25-27</sup> However, the UPR plays other roles in B cells, independent of its requirement to support increased secretory Ig synthesis *per se*, including for differentiation beyond the pro-B-cell stage.<sup>24</sup> In mature B cells, differentiation-promoting factors, such as IL4 or LPS, rapidly activate a subset of UPR components prior to increased Ig synthesis and the UPR is activated normally in cells that lack the ability to secrete IgM.<sup>23,28-30</sup> BCR stimulation has also been shown to increase some UPR components although this stimulation alone is not sufficient to promote differentiation.<sup>31</sup> Thus, UPR activation is not simply a consequence of stress, but can be a signal-regulated pathway that induces a partial, “anticipatory” response which prepares B cells for subsequent antibody production. In contrast to these physiological pro-survival responses, prolonged, high-level UPR activation in response to pharmacological agents (such as proteasome inhibitors which cause accumulation of mis-folded proteins) induces a cell death-promoting UPR response.<sup>19,20</sup>

Previous studies have shown that CLL cells express some UPR components and that pharmacological inducers of the UPR promote apoptosis of CLL cells *in vitro*.<sup>32-36</sup> However, the potential regulation of the UPR following BCR stimulation of CLL cells has not been studied. In this paper, we demonstrate for the first time that sIgM stimulation results in a “partial” activation of the UPR, with selective activation of specific downstream UPR effector pathways. Higher levels of UPR activation correlated with more aggressive disease and BCR-targeted kinase inhibitors decreased UPR activation suggesting that this response may contribute to disease progression and that its inhibition may be important for clinical activity of drugs such as ibrutinib.

## **Materials and methods**

### *Patients and cell samples*

Patients were recruited after written informed consent was provided in accordance with Ethics Committee approvals and the Declaration of Helsinki. Blood was obtained from patients with IgM<sup>+</sup>IgD<sup>+</sup> CLL with a diagnostic phenotype who attended Hematology outpatient clinics at the Leicester Royal Infirmary, Portsmouth Hospital, Southampton General Hospital, the Royal Wolverhampton Hospitals NHS Trust or the Royal Berkshire Hospital, Reading (all UK). Clinical

details for the patients studied are given in **Supplementary Table 1**. The majority of samples were obtained at or shortly after diagnosis and mainly prior to any therapy for CLL. Where treatment for CLL had taken place, this was at least 6 months prior to sample collection. Disease was considered to be more aggressive if there were signs of clinical progression and/or the patient was treated for CLL at any point following diagnosis.

Blood samples were processed as previously described.<sup>11</sup> Cell viability determined by trypan blue exclusion was  $\geq 90\%$ . The proportion of CD5<sup>+</sup>CD19<sup>+</sup> CLL cells was  $>80\%$  in all cases. *IGHV* mutation status, expression of cell surface CD5, CD19 and CD38, and ZAP70 were determined as previously described.<sup>11,37</sup> IgM signaling capacity was determined by measuring the percentage of cells with increased intracellular calcium following stimulation with soluble goat F(ab')<sub>2</sub> anti-IgM and using a cut-off value of  $\geq 5\%$  responding cells to define samples as sIgM responsive.<sup>11</sup> Normal B cells were isolated from peripheral blood or buffy coats from healthy donors using the B cell Isolation Kit II with the addition of anti-CD138 Microbeads (both Miltenyi Biotec, Bisley, UK) to ensure effective depletion of plasma cells.

**Additional methods are provided as supplementary material.**

## Results

### *“Basal” activation of UPR-associated pathways in CLL and normal B cells*

We first analyzed “basal” activation of the UPR (ie, in unstimulated cells) in CLL samples isolated from the blood of 40 patients using Q-PCR to quantify expression of *XBP1* and *CHOP* RNAs. The samples comprised 20 U-CLL which, as previously described,<sup>11</sup> generally retained sIgM signaling responsiveness. We also analyzed 20 M-CLL samples. These samples were selected to contain a substantial proportion of sIgM signal-competent samples to allow us to probe potential correlations between UPR activation and sIgM signaling within this subset. Circulating B cells from healthy individuals were analyzed as controls. To validate the Q-PCR assays, CLL samples were treated with the pharmacological UPR inducer thapsigargin. As expected, thapsigargin substantially increased *XBP1* and *CHOP* RNA expression in CLL samples (**Supplementary Figure 2A**).

Although basal expression of *CHOP* and *XBP1* RNAs were variable between individual CLL samples, median *CHOP* and *XBP1* RNA expression levels were significantly higher than normal B cells (**Figure 1A**). *CHOP* and *XBP1* RNA expression levels were closely correlated demonstrating that these RNAs are generally co-expressed in individual CLL samples (**Figure 1B**).

We extended these results by examining other features of UPR activation in unstimulated CLL cells including BIP, PERK and the PERK substrate eIF2 $\alpha$ . We were unable to identify antibodies suitable for reliable analysis of XBP1 and CHOP protein expression in CLL cells. As expected, thapsigargin increased BIP protein expression, and phosphorylation of PERK (detected by reduced migration) and eIF2 $\alpha$  (detected using a phospho-specific antibody) (**Supplementary Figure 2B**). Immunoblotting demonstrated that basal expression of BIP protein was elevated in some CLL samples compared to normal B cells (**Figure 1C**). We also detected moderately increased PERK expression in some CLL samples compared to normal B cells but not a clear decrease in PERK mobility as observed in thapsigargin-treated CLL cells. Consistent with weak PERK activation in CLL cells, we detected only very modest levels eIF2 $\alpha$  phosphorylation in some samples.

Although we detected raised *XBP1* RNA in unstimulated CLL samples, there was little evidence for accumulation of *XBP1S*; very low levels of basal expression of *XBP1S* RNA were detected in only 2/18 untreated CLL cell samples (not shown). *XBP1S* expression was detected in thapsigargin-treated cells confirming the validity of the assay. However, even in thapsigargin-treated cells, *XBP1S* RNA levels were relatively low level (**Supplementary Figure 3**).

Overall, these results demonstrate substantial but variable basal activation of some UPR components in CLL blood cells.

#### *Correlations between basal UPR activation and sIgM signaling capacity in vitro*

We next investigated potential correlations between basal UPR activation and sIgM signaling capacity measured using anti-IgM-induced intracellular Ca<sup>2+</sup> mobilization. When considering the total cohort, there were significant correlations between sIgM signaling capacity *in vitro* and *CHOP* and *XBP1* RNA expression levels with higher basal level expression of these RNAs associated with retained sIgM signaling capacity (**Figure 2A,B**). Similar to the complete cohort, there was a positive correlation between signaling capacity and *CHOP* RNA levels when U-CLL and M-CLL samples were considered separately (**Figure 2C,E**). There was a similar trend for *XBP1* RNA but this did not reach statistical significance (**Figure 2D,F**). Thus, basal UPR activation correlates with sIgM signaling capacity *in vitro*, in both the M-CLL and U-CLL subsets. Consistent with the correlation between UPR activation and retained signal capacity, there were trends towards increased *CHOP/XBP1* RNA expression in U-CLL (**Supplementary Figure 4**). However, it is important to emphasize, that these differences did not reach statistical significance, most likely due to the enrichment for M-CLL signal competent samples in the current cohort.

#### *Correlation between basal UPR activation and clinical behavior*

To begin to probe the potential clinical significance of UPR activation, we also investigated whether variable basal UPR activation correlated with clinical behavior depending on whether the patient had indolent or more aggressive disease (see Materials and methods). Higher basal *CHOP* or *XBP1* RNA levels were associated with more aggressive disease in the total cohort (**Figure 3A,B**). Similar correlations were detected when only Binet stage A disease (U-CLL and M-CLL combined) was analyzed (n=23) (**Figure 3C,D**). There was also consistently higher expression of *CHOP* or *XBP1* RNAs in more aggressive disease compared to indolent disease specifically within the M-CLL subset (all stages) although this was only significant for *XBP1* (**Figure 3E,F**). There were only two cases of indolent disease amongst the 17 U-CLL samples analyzed where outcome data was available precluding meaningful analysis of this subset. These observations provide further support for the idea that high basal UPR activation is associated with retained sIgM signaling and that these features may be associated with relatively aggressive disease, possibly even within M-CLL.

#### *Effect of sIgM engagement on UPR activation*

The correlation between basal UPR activation and retained sIgM signaling capacity suggested that UPR activation was directly linked to the capacity to respond to antigen stimulation *in vivo*. Activation of sIgM *in vitro* using anti-IgM antibodies mimics positive BCR signaling in CLL. Therefore, to determine directly whether sIgM stimulation activated the UPR in CLL cells, we investigated the effects of anti-IgM on *XBP1/CHOP* RNA expression. Normal B cells were analyzed as controls.

In normal B cells, soluble anti-IgM increased expression of *CHOP* RNA most strongly at 1 hour and less so at 6 hours post-stimulation (**Figure 4A**). Induction of *XBP1* RNA was greatest at 6 hours post-stimulation. Similar experiments were performed using CLL samples all of which were classed as sIgM signal responsive. There were significant increases in *CHOP* and *XBP1* RNA expression following treatment with soluble anti-IgM compared to control cells (**Figure 4B**). However, similar to other sIgM signaling responses,<sup>38</sup> increases in *CHOP/XBP1* RNAs were much weaker than in normal B cells.

The weak induction of *CHOP/XBP1* RNAs in CLL samples may reflect the low level of sIgM expression in these cells, a consequence of anergy-promoting interactions *in vivo*.<sup>7,11</sup> Since BCR signal strength in CLL cells can be enhanced by treating cells with immobilized anti-IgM<sup>16</sup> we also stimulated sIgM signal responsive CLL samples with anti-IgM bound to Dynabeads (**Figure 4B**). Cells were analyzed at 6 hours post-stimulation since the onset of signaling is delayed in cells treated with bead-bound<sup>9</sup> compared to soluble antibodies,<sup>17</sup> presumably due to potentially slower engagement of sIgM. Compared to soluble antibodies, bead-bound anti-IgM triggered larger increases in *CHOP/XBP1* RNA expression

(**Figure 4B**). Considering all data for anti-IgM treated cells, there was a strong positive correlation between induction of *XBP1* and *CHOP* RNAs (**Figure 4C**). Consistent with the stronger signal, increases in phosphorylation of ERK1/2 and AKT was greater and longer-lasting in cells treated with bead-bound compared to soluble anti-IgM (**Supplementary Figure 5**). There was considerable variation in the extent of anti-IgM-induced *CHOP/XBP1* RNA expression (**Figure 4B**). However, the fold increase in *CHOP* or *XBP1* RNA expression did not differ between M-CLL and U-CLL in this cohort of signaling competent samples, and did not correlate with ZAP-70 expression or sIgM expression (data not shown).

We performed similar experiments to determine whether anti-IgM also induced protein markers of the UPR in CLL using 15 signaling responsive samples. Treatment with anti-IgM increased expression of both PERK and BIP (**Figure 5A,B**). The induction by soluble anti-IgM was significant for some time points, however, levels of induction were greater for bead-bound anti-IgM. Similar to *CHOP/XBP1* RNAs, there was considerable variation in the extent of anti-IgM-induced PERK/BIP expression (**Figure 5A,B**) although these parameters correlated closely within individual samples indicating co-regulation (**Figure 5C**). As expected, anti-IgM also induced ERK1/2 phosphorylation (**Figure 5A**). Thapsigargin also induced ERK1/2 phosphorylation in a subset of samples.

Variable induction of PERK/BIP was not clearly different between M-CLL and U-CLL samples and did not correlate with ZAP-70 expression or sIgM expression. However, variation in the extent of PERK/BIP induction did appear to be related to “strength” of sIgM-induced signaling analyzed using other read-outs. First, there was no evidence for induction of PERK or BIP expression in 4 non-responsive samples (**Supplementary Figure 6**). Second, there was a modest, but significant correlation between anti-IgM-induced ERK1/2 phosphorylation and BIP/PERK induction in a subset of signal responsive samples (**Supplementary Figure 7**). sIgM stimulation also increased BIP and PERK expression in normal B cells, although analysis was technically difficult due to the small number of B cells obtained for immunoblot analysis (**Supplementary Figure 8**). Similar to unstimulated cells, we did not detect increased *XBP1S* expression in CLL cells treated with anti-IgM (data not shown).

#### *Expression of UPR associated components in vivo*

We performed immunohistochemistry to investigate UPR activation in the LN of patients with CLL/small lymphocytic lymphoma (SLL) (**Figure 6** and **Supplementary Table 2**). Because of the absence of suitable antibodies, analysis was restricted to PERK and XBP1. Comparisons were made to multiple myeloma, known to be associated with UPR activation.<sup>39</sup>

Overall, PERK and XBP1 were widely detected in LNs samples; 11/11 and 10/11 samples were positive for PERK and XBP1 expression, respectively.



Similar to myeloma samples, PERK immunostaining was largely extranuclear, consistent with ER-localization. In CLL, PERK was more strongly expressed in cells within PCs compared to surrounding cells in 6/11 samples. In 1 additional sample, expression was only detected in malignant cells within PCs. In the other samples, PERK expression was not different between cells within and outside of PCs. There was also variability in the distribution of XBP1 between individual samples, but two broad patterns of expression were observed. In 5/10 positive samples, XBP1 was predominantly detected in the nucleus (similar to the localization in myeloma samples) in cells outside of PCs. In the other positive samples, XBP1 expression was predominantly localized outside of the nucleus and in these samples, expression was mainly detected in leukemic blasts within PCs. Overall, the analysis demonstrates that UPR-associated proteins were expressed within malignant LNs. Although there was substantial intrasample variation, features were frequently more prominent in cells within PCs consistent with the idea that UPR activation in CLL cells is a consequence of antigen engagement *in vivo*. Clinical data and/or matched blood samples were not available for these samples, so we were unable to correlate this variation to outcome or variable sIgM signaling capacity.

To explore further potential regulation of the UPR *in vivo*, we analyzed expression of *BIP*, *CHOP* and *XBP1* RNAs using GEA data from a study comparing CLL cells derived from blood and LN.<sup>40</sup> The three RNAs were more highly expressed in LN samples compared to blood. Differences were significant (paired Student's t-tests) for *BIP* and *CHOP* ( $P < 0.0001$  and  $P = 0.0014$ , respectively), but not for *XBP1* ( $P = 0.8995$ ).

#### *Effect of BCR signaling inhibitors on UPR regulation*

To investigate whether UPR induction was a direct consequence of activation of signaling pathways, CLL cells were pre-treated with inhibitors of BCR associated kinases prior to stimulation with bead-bound anti-IgM. The inhibitors tested were the clinical BTK and SYK inhibitors ibrutinib and tamsitinib (the active form of fostamatinib). Both compounds significantly reduced anti-IgM-induced BIP and PERK expression (**Figure 7**). As expected, both inhibitors also effectively blocked induction of phosphorylation of both AKT and ERK1/2 (**Figure 7**). Thus, sIgM-induced UPR activation appears to be mediated via kinase-dependent signaling pathways and its inhibition may contribute to the therapeutic activity of agents such as ibrutinib.

## **Discussion**

BCR signaling has emerged as a key determinant of the clinical behavior of CLL and as an effective target for therapeutic attack. It is important, therefore, to

define the functional consequences of sIgM stimulation. In this work we investigated potential links between the BCR and the UPR, a multifunctional response pathway which can promote cell survival or death, dependent on the extent and duration of the activating signal. Several studies have shown that pharmacological inducers of the UPR promote apoptosis of CLL cells *in vitro*.<sup>33,34,36</sup> However, the potential regulation of the UPR following BCR stimulation of CLL cells has not been studied previously.

Our results demonstrate that sIgM stimulation results in activation of a partial UPR. This conclusion is based on three lines of evidence. First, variable levels of basal activation of the UPR in unstimulated, circulating CLL cells correlated closely with sIgM signal capacity and were associated with more aggressive disease. Second, stimulation of sIgM *in vitro* increased expression of UPR components and this was effectively blocked by BCR-targeted kinase inhibitors, including ibrutinib. Third, immunohistochemistry and GEA analysis demonstrated relatively high levels of UPR components in LNs *in vivo*. Interestingly, activation and therapeutic targeting of the UPR has also been reported during leukemogenesis in the E $\mu$ -*TCL1* mouse model of CLL,<sup>35,41</sup> although the relevance of antigen signaling *in vivo* in this model remains unclear.

Our analysis demonstrated that sIgM stimulation, especially using bead-bound anti-IgM, triggered UPR induction using signal-responsive samples from both the M-CLL and U-CLL subsets. By contrast, anti-IgM did not significantly induce UPR activation in non-signaling samples indicating that the competency for UPR induction broadly correlates with sIgM signaling responsiveness measured using canonical read-outs. There was variation in the extent of UPR induction within the signal-responsive samples. Although this did not obviously correlate with *IGHV* mutation status, ZAP-70 expression or sIgM expression, there did appear to be a correlation between variable BIP/PERK induction and the “strength” of sIgM signaling (measured by parallel analysis of ERK1/2 phosphorylation) amongst signal-responsive samples. Further studies are required to probe relationships between sIgM-induced UPR activation and other signaling responses, however, UPR induction is likely to be part of a constellation of responses, co-regulated downstream of sIgM in signal-responsive samples.<sup>4</sup> Consistent with this, pre-treatment of samples with ibrutinib or tamatinib effectively inhibited anti-IgM-induced UPR activation, providing functional evidence for linkage between kinase activation and UPR activation. We did not address consequences of sIgD stimulation in this study but have shown previously that, although competent for triggering initial calcium responses, anti-IgD fails to effectively engage downstream responses.<sup>17</sup> Consistent with this, a recent GEA study showed that *BIP* RNA was induced in CLL samples following stimulation of sIgM, but not sIgD.<sup>42</sup>

An important finding of the study was that UPR activation in CLL cells was partial. There was clear evidence for increased expression of *CHOP* and *XBP1* RNAs, and BIP protein. However, the PERK arm appeared to be only weakly

activated since PERK expression was increased, but without substantial phosphorylation, and there were only modest levels of phosphorylation of its substrate eIF2 $\alpha$ . Despite the induction of full length *XBP1* RNA, there was little evidence for IRE1-dependent processing to *XBP1S*, consistent with a previous study demonstrating only low expression of *XBP1S* protein in CLL/SLL LN.<sup>43</sup> Treatment of CLL cells with thapsigargin resulted in activation of all arms of the UPR. Thus, failure to activate some specific parts of the UPR likely represents the consequences of selective regulation rather than inherent defects which prevent induction of these specific arms. However, it was noticeable that *XBP1S* splicing was low, even in thapsigargin-treated cells, consistent with the idea that activation of this pathway may be relatively weak in CLL.<sup>33</sup>

Direct analysis of the functional consequences of UPR activation was not explored in this work; this would require knockdown of multiple proteins which is technically difficult in any cell system, especially in CLL where RNA interference (RNAi) is extremely demanding. However, the molecular hallmarks of the partial UPR activation in CLL cells is very reminiscent of the “anticipatory” UPR that has been described in normal B cells. In this situation, selective activation of some UPR components is thought to prepare the cells for subsequent immunoglobulin secretion. For example, *CHOP* and *XBP1* RNAs are induced within 1-2 hours following treatment of mouse B cells with IL4, whereas *XBP1S* splicing is detected much later at 48 hours post-treatment and is dependent on enhanced Ig production.<sup>44</sup>

As in normal B cells, the partial UPR activation in CLL cells is likely to have a pro-survival function. First, anti-IgM-induced UPR activation in CLL cells lacks components typically associated with pro-apoptotic responses. IRE1 is the principle mediator of UPR-associated apoptosis, via downstream activation of pro-apoptotic kinases such as ASK1 and JNK (**Supplementary Figure 1**). However, the absence of substantial *XBP1S* splicing, which is catalyzed by IRE1’s endonuclease activity, indicates that IRE1 is not effectively activated in CLL cells. Moreover, anti-IgM stimulation only very weakly induces JNK phosphorylation in CLL cells.<sup>16</sup> Although *CHOP* is commonly considered as a pro-apoptotic factor, analysis of *Chop*-deficient mouse B cells has clearly demonstrated that CHOP does not play a pro-apoptotic role in B cells.<sup>31,45</sup> Second, UPR activation in CLL cells is associated with increased expression of BIP, a chaperone with pro-survival functions.<sup>46</sup> For example, in diffuse large B-cell lymphoma, high level of BIP expression is associated with poor prognosis and its overexpression confers resistance to apoptosis *in vitro*.<sup>47</sup> BIP is induced in normal murine T cells following stimulation *in vitro* and its ablation using RNAi promotes apoptosis in mouse EL4 T-lymphoma cells.<sup>48</sup> The conclusion that partial UPR activation in CLL cells promotes survival is consistent with the previous observation that RNAi-mediated knock-down of BIP promotes CLL cell apoptosis *in vitro*.<sup>32</sup> However, it is possible that UPR activation has additional functional consequences. For example, *Xbp1* is required for optimal signaling via

slgM and CXCR4, although the functional basis for these effects are unknown.<sup>28,41</sup>

The close correlation between basal UPR activation and retained slgM signal capacity supports the idea that UPR activation is not simply an artifact of stimulation *in vitro*, but can also be a consequence of antigen engagement *in vivo*. Although antigen engagement is thought to be on-going in all CLL, distinct biological responses appear to determine clinical behavior.<sup>1</sup> Antigen-induced anergy is associated with strong down-modulation of slgM signaling and is most prominent in M-CLL.<sup>11</sup> By contrast, positive signaling is generally more evident in U-CLL and is associated with retained signaling capacity.<sup>11</sup> Although the overall behavior of U-CLL and M-CLL is distinct, there is heterogeneity within these subsets, especially within M-CLL,<sup>11</sup> and high levels of retained signaling in M-CLL may highlight cases at higher risk of progression.<sup>18</sup> Overall, UPR activation appears to be one of several markers detected in circulating cells that reveal prior positive signaling within tissues (**Supplementary Figure 9**). By contrast, strong downmodulation of slgM signaling responses *in vitro* (including reduced capacity to enhance UPR activation) and lower levels of “basal” UPR activation are associated with anergy. Activation of an “anticipatory” UPR is linked to differentiation and this linkage between anergy and reduced slgM-induced UPR activation is consistent with the observation that differentiation responses are reduced in anergic cells in non-malignant model systems<sup>7</sup>. Moreover, very recent data demonstrate that IL21-induced differentiation responses are suppressed in anergic CLL cells.<sup>49</sup> Further studies will be required to more accurately define the relationship between UPR activation, slgM signal capacity and disease behavior in larger, unselected cohorts. However, the expression of UPR components, along with other markers such as MYC and MCL1 which are also induced following slgM-stimulation *in vitro* may have utility as prognostic or predictive markers, including for new BCR-targeted kinase inhibitors, possibly including within the M-CLL subset.

In summary, our studies have led to the novel observation that slgM stimulation in CLL cells results in partial activation of the UPR. UPR activation appears to contribute to the growth promoting effects of BCR stimulation and is associated with more aggressive disease. Inhibition of UPR activation may contribute to the therapeutic effects of novel drugs targeted towards BCR-associated signaling kinases, including BTK and SYK.

## Acknowledgements

We are extremely grateful to the patients involved in this study for the kind gift of samples. We are very grateful for the generous support of Drs Simon Wagner, Robert Corser, Abraham Jacob and Henri Grech and their associated clinical teams. We are also grateful for the technical support of Isla Henderson and Ian

Tracy. This work was supported by the Kay Kendall Leukaemia Fund, Leukaemia and Lymphoma Research, Worldwide Cancer Research, Cancer Research UK, the Southampton Experimental Cancer Medicine Centre and the University of Southampton. MSH gratefully acknowledges support from a Postgraduate National Program of José Castillejo fellowship and financial sponsorship from the Spanish Ministry of Education.

### **Author contributions**

SK, VC, MSH, AL and MC performed research and analyzed data; SK, AJS, MAK, FKS and GP designed the research and analyzed data; KNP, BK, ASD, FF provided patient samples and analyzed clinical data; SK and GP wrote the initial draft of the manuscript; and all authors contributed to the modification of the draft and approved the final submission.

### **Conflict-of-interest disclosure**

The authors declare no competing financial interests.

## References

1. Stevenson FK, Krysov S, Davies AJ, Steele AJ, Packham G. B-cell receptor signaling in chronic lymphocytic leukemia. *Blood*. 2011;118(16):4313-4320.
2. Woyach JA, Johnson AJ, Byrd JC. The B-cell receptor signaling pathway as a therapeutic target in CLL. *Blood*. 2012;120(6):1175-1184.
3. Zhang S, Kipps TJ. The Pathogenesis of Chronic Lymphocytic Leukemia. *Annu Rev Pathol*. 2013.
4. Packham G, Krysov S, Allen A, et al. The outcome of B-cell receptor signaling in chronic lymphocytic leukemia: proliferation or anergy. *Haematologica*. 2014;99(7):1138-1148.
5. Forconi F, Potter KN, Wheatley I, et al. The normal IGHV1-69-derived B-cell repertoire contains stereotypic patterns characteristic of unmutated CLL. *Blood*. 2010;115(1):71-77.
6. Seifert M, Sellmann L, Bloehdorn J, et al. Cellular origin and pathophysiology of chronic lymphocytic leukemia. *J Exp Med*. 2012;209(12):2183-2198.
7. Cambier JC, Gauld SB, Merrell KT, Vilen BJ. B-cell anergy: from transgenic models to naturally occurring anergic B cells? *Nat Rev Immunol*. 2007;7(8):633-643.
8. Byrd JC, Furman RR, Coutre SE, et al. Targeting BTK with ibrutinib in relapsed chronic lymphocytic leukemia. *N Engl J Med*. 2013;369(1):32-42.
9. Coelho V, Krysov S, Steele A, et al. Identification in CLL of circulating intracлонаl subgroups with varying B-cell receptor expression and function. *Blood*. 2013;122(15):2664-2672.
10. Calissano C, Damle RN, Marsilio S, et al. Intracлонаl complexity in chronic lymphocytic leukemia: fractions enriched in recently born/divided and older/quiescent cells. *Mol Med*. 2011;17(11-12):1374-1382.
11. Mockridge CI, Potter KN, Wheatley I, Neville LA, Packham G, Stevenson FK. Reversible anergy of sIgM-mediated signaling in the two subsets of CLL defined by VH-gene mutational status. *Blood*. 2007;109(10):4424-4431.
12. Muzio M, Apollonio B, Scielzo C, et al. Constitutive activation of distinct BCR-signaling pathways in a subset of CLL patients: a molecular signature of anergy. *Blood*. 2008;112(1):188-195.
13. Apollonio B, Scielzo C, Bertilaccio MT, et al. Targeting B-cell anergy in chronic lymphocytic leukemia. *Blood*. 2013;121(19):3879-3888.
14. Zhang W, Kater AP, Widhopf GF, 2nd, et al. B-cell activating factor and v-Myc myelocytomatosis viral oncogene homolog (c-Myc) influence progression of chronic lymphocytic leukemia. *Proc Natl Acad Sci U S A*. 2010;107(44):18956-18960.
15. Pepper C, Lin TT, Pratt G, et al. Mcl-1 expression has in vitro and in vivo significance in chronic lymphocytic leukemia and is associated with other poor prognostic markers. *Blood*. 2008;112(9):3807-3817.

16. Petlickovski A, Laurenti L, Li X, et al. Sustained signaling through the B-cell receptor induces Mcl-1 and promotes survival of chronic lymphocytic leukemia B cells. *Blood*. 2005;105(12):4820-4827.
17. Krysov S, Dias S, Paterson A, et al. Surface IgM stimulation induces MEK1/2-dependent MYC expression in chronic lymphocytic leukemia cells. *Blood*. 2012;119(1):170-179.
18. Paterson A, Mockridge CI, Adams JE, et al. Mechanisms and clinical significance of BIM phosphorylation in chronic lymphocytic leukemia. *Blood*. 2012;119(7):1726-1736.
19. Walter P, Ron D. The unfolded protein response: from stress pathway to homeostatic regulation. *Science*. 2011;334(6059):1081-1086.
20. Hetz C. The unfolded protein response: controlling cell fate decisions under ER stress and beyond. *Nat Rev Mol Cell Biol*. 2012;13(2):89-102.
21. Todd DJ, Lee AH, Glimcher LH. The endoplasmic reticulum stress response in immunity and autoimmunity. *Nat Rev Immunol*. 2008;8(9):663-674.
22. Reimold AM, Iwakoshi NN, Manis J, et al. Plasma cell differentiation requires the transcription factor XBP-1. *Nature*. 2001;412(6844):300-307.
23. Iwakoshi NN, Lee AH, Glimcher LH. The X-box binding protein-1 transcription factor is required for plasma cell differentiation and the unfolded protein response. *Immunol Rev*. 2003;194:29-38.
24. Zhang K, Wong HN, Song B, Miller CN, Scheuner D, Kaufman RJ. The unfolded protein response sensor IRE1 $\alpha$  is required at 2 distinct steps in B cell lymphopoiesis. *J Clin Invest*. 2005;115(2):268-281.
25. Lee AH, Iwakoshi NN, Anderson KC, Glimcher LH. Proteasome inhibitors disrupt the unfolded protein response in myeloma cells. *Proc Natl Acad Sci U S A*. 2003;100(17):9946-9951.
26. Carrasco DR, Sukhdeo K, Protopopova M, et al. The differentiation and stress response factor XBP-1 drives multiple myeloma pathogenesis. *Cancer Cell*. 2007;11(4):349-360.
27. Aronson LI, Davies FE. DangER: protein ovERload. Targeting protein degradation to treat myeloma. *Haematologica*. 2012;97(8):1119-1130.
28. Hu CC, Dougan SK, McGehee AM, Love JC, Ploegh HL. XBP-1 regulates signal transduction, transcription factors and bone marrow colonization in B cells. *EMBO J*. 2009;28(11):1624-1636.
29. Gass JN, Gifford NM, Brewer JW. Activation of an unfolded protein response during differentiation of antibody-secreting B cells. *J Biol Chem*. 2002;277(50):49047-49054.
30. van Anken E, Romijn EP, Maggioni C, et al. Sequential waves of functionally related proteins are expressed when B cells prepare for antibody secretion. *Immunity*. 2003;18(2):243-253.
31. Skalet AH, Isler JA, King LB, Harding HP, Ron D, Monroe JG. Rapid B cell receptor-induced unfolded protein response in nonsecretory B cells correlates with pro- versus antiapoptotic cell fate. *J Biol Chem*. 2005;280(48):39762-39771.
32. Rosati E, Sabatini R, Rampino G, et al. Novel targets for endoplasmic reticulum stress-induced apoptosis in B-CLL. *Blood*. 2010;116(15):2713-2723.

33. Lust S, Vanhoecke B, M VG, et al. Xanthohumol activates the proapoptotic arm of the unfolded protein response in chronic lymphocytic leukemia. *Anticancer Res.* 2009;29(10):3797-3805.
34. Carew JS, Nawrocki ST, Krupnik YV, et al. Targeting endoplasmic reticulum protein transport: a novel strategy to kill malignant B cells and overcome fludarabine resistance in CLL. *Blood.* 2006;107(1):222-231.
35. Kriss CL, Pinilla-Ibarz JA, Mailloux AW, et al. Overexpression of TCL1 activates the endoplasmic reticulum stress response: a novel mechanism of leukemic progression in mice. *Blood.* 2012;120(5):1027-1038.
36. Mahoney E, Maddocks K, Flynn J, et al. Identification of endoplasmic reticulum stress-inducing agents by antagonizing autophagy: a new potential strategy for identification of anti-cancer therapeutics in B-cell malignancies. *Leuk Lymphoma.* 2013;54(12):2685-2692.
37. Lanham S, Hamblin T, Oscier D, Ibbotson R, Stevenson F, Packham G. Differential signaling via surface IgM is associated with VH gene mutational status and CD38 expression in chronic lymphocytic leukemia. *Blood.* 2003;101(3):1087-1093.
38. Efremov DG, Gobessi S, Longo PG. Signaling pathways activated by antigen-receptor engagement in chronic lymphocytic leukemia B-cells. *Autoimmun Rev.* 2007;7(2):102-108.
39. Vincenz L, Jager R, O'Dwyer M, Samali A. Endoplasmic reticulum stress and the unfolded protein response: targeting the Achilles heel of multiple myeloma. *Mol Cancer Ther.* 2013;12(6):831-843.
40. Herishanu Y, Perez-Galan P, Liu D, et al. The lymph node microenvironment promotes B-cell receptor signaling, NF-kappaB activation, and tumor proliferation in chronic lymphocytic leukemia. *Blood.* 2011;117(2):563-574.
41. Tang CH, Ranatunga S, Kriss CL, et al. Inhibition of ER stress-associated IRE-1/XBP-1 pathway reduces leukemic cell survival. *J Clin Invest.* 2014;124(6):2585-2598.
42. Tavolaro S, Peragine N, Chiaretti S, et al. IgD cross-linking induces gene expression profiling changes and enhances apoptosis in chronic lymphocytic leukemia cells. *Leuk Res.* 2013;37(4):455-462.
43. Maestre L, Tooze R, Canamero M, et al. Expression pattern of XBP1(S) in human B-cell lymphomas. *Haematologica.* 2009;94(3):419-422.
44. Iwakoshi NN, Lee AH, Vallabhajosyula P, Otipoby KL, Rajewsky K, Glimcher LH. Plasma cell differentiation and the unfolded protein response intersect at the transcription factor XBP-1. *Nat Immunol.* 2003;4(4):321-329.
45. Masciarelli S, Fra AM, Pengo N, et al. CHOP-independent apoptosis and pathway-selective induction of the UPR in developing plasma cells. *Mol Immunol.* 2010;47(6):1356-1365.
46. Li J, Lee AS. Stress induction of GRP78/BiP and its role in cancer. *Curr Mol Med.* 2006;6(1):45-54.
47. Mozos A, Roue G, Lopez-Guillermo A, et al. The expression of the endoplasmic reticulum stress sensor BiP/GRP78 predicts response to chemotherapy and determines the efficacy of proteasome inhibitors in diffuse large b-cell lymphoma. *Am J Pathol.* 2011;179(5):2601-2610.



48. Takano S, Ando T, Hiramatsu N, et al. T cell receptor-mediated signaling induces GRP78 expression in T cells: the implications in maintaining T cell viability. *Biochem Biophys Res Commun.* 2008;371(4):762-766.
49. Duckworth A, Glenn M, Slupsky JR, Packham G, Kalakonda N. Variable induction of PRDM1 and differentiation in chronic lymphocytic leukemia is associated with anergy. *Blood.* 2014;123(21):3277-3285.

## Figure legends

### Figure 1. Expression of UPR components in unstimulated CLL samples and normal B cells

(A) *CHOP* and *XBP1* RNA expression was quantified by Q-PCR in CLL samples (n=40) and normal B cells (n=7). Expression values were normalized so that the average value in normal B cells was set to 1.0. Graphs show median and individual data points, and the statistical significance of differences between CLL samples and normal B cells (Mann-Whitney test). (B) Correlation between *CHOP* and *XBP1* RNA expression in CLL samples. The line shows results of linear regression and the statistical significance of the correlation is shown (Spearman correlation). (C) Immunoblot analysis of BIP, total and phospho-eIF2 $\alpha$ , PERK and GAPDH (loading control) in normal B cells (2 preparations shown) and CLL samples. Results shown are representative of more than 30 samples studied across a series of separate immunoblots.

### Figure 2. Correlations between *CHOP* and *XBP1* RNA expression and sIgM signaling capacity

Correlations between basal *CHOP* and *XBP1* RNA expression and anti-IgM signaling responsiveness in (A,B) all samples, (C,D) M-CLL and (E,F) U-CLL. The statistical significance of differences was analyzed using the Mann-Whitney test.

### Figure 3. Correlations between *CHOP* and *XBP1* RNA expression and clinical behavior

Correlations between basal *CHOP* and *XBP1* RNA expression and indolent/aggressive disease for (A,B) all CLL/all stages (n=31), (C,D) stage A (M-CLL and U-CLL combined) (n=23) and (E,F) M-CLL (all stages) (n=19). The statistical significance of differences was analyzed using Mann-Whitney test.

### Figure 4. Regulation of *CHOP* and *XBP1* RNA expression by anti-IgM

(A) Normal B cells and (B) CLL samples were stimulated with soluble (sol) or bead-bound (bead) anti-IgM for 1 or 6 h and expression of *CHOP* and *XBP1* RNAs analyzed by Q-PCR. Expression values were normalized so that the average value in control normal and CLL cells was set to 1.0. Graphs show mean values ( $\pm$ SD) for data obtained with 6 or 4 preparations of normal B cells (for *CHOP* and *XBP1* analysis, respectively). For experiments with CLL, 15 samples were used to compare responses between soluble anti-IgM at 1 and 6 hours and 10 further samples were used to compare responses to soluble and bead-bound anti-IgM. The statistical significance of differences between treated and control cells are shown for each condition (Student's t-test). (C) Correlation between fold induction of *XBP1* and *CHOP* RNAs in soluble/bead-bound anti-IgM treated CLL samples (1 and 6 hour data combined; linear regression and Spearman correlation shown).

### Figure 5. Regulation of BIP and PERK expression by anti-IgM

CLL samples (n=15) were stimulated with soluble (sol) or bead-bound (bead) anti-IgM, or thapsigargin as a control (TG; 15  $\mu$ M) for up to 24 hours and expression of PERK, BIP and phosphorylated ERK1/2 was analyzed by immunoblotting. (A) Representative results from 2 CLL samples. Phosphorylated and non-phosphorylated forms of PERK are indicated by white and black triangles, respectively. (B) Quantitation of results. Expression values were normalized so that the average value in control cells at each time point was set to 1.0 and graphs show mean values ( $\pm$ SD). The statistical significance of differences is shown. Vertical values show the *P* values for difference between that condition and control cells whereas horizontal values show *P* values for the differences between soluble and bead-bound anti-IgM-treated samples at each time point (paired Student's t-test). (C) Correlation between fold induction of PERK and BIP in soluble/bead-bound anti-IgM-treated CLL samples (3, 6 and 24 hours data combined; linear regression and Spearman correlation shown).

### **Figure 6. UPR activation in CLL/SLL lymph nodes**

Immunohistochemical analysis of expression of (A,C,F) PERK, (B,D,G) XBP1 and (E,H) Ki-67 in (A,B) multiple myeloma and (C-H) CLL/SLL lymph nodes. Original magnification of images are shown. Results are representative of a total of 11 biopsies analyzed. CLL PCs are circled and higher magnification images of the PC marked (\*) in C and D are shown in F and G. The insert in G shows the nuclear expression of XBP1 in the small CLL cells in contrast to the cytoplasmic expression in the large blasts in the proliferation centres. Arrows highlight large blasts in F and G. Images for C and F (PERK), and D and G (XBP1) are from samples 8 and 11, respectively. Inset shown in G is from sample 1.

### **Figure 7. Effect of signaling inhibitors on anti-IgM-induced UPR activation**

Cells were pre-treated with DMSO, ibrutinib or tamatinib for 30 minutes before being stimulated with bead-bound anti-IgM or control antibodies. Expression of PERK, BIP, phosphorylated ERK1/2 and phosphorylated AKT was analyzed at 24 hours. (A) Representative immunoblots. (B) Quantitation of results for all samples (n=6 for ibrutinib and tamatinib). Graphs show inhibition of PERK/BIP expression with anti-IgM/DMSO treated cells set to 100%. The statistical significance of differences between control and compound-treated control cells is shown (Student's t-test).

Figure 1

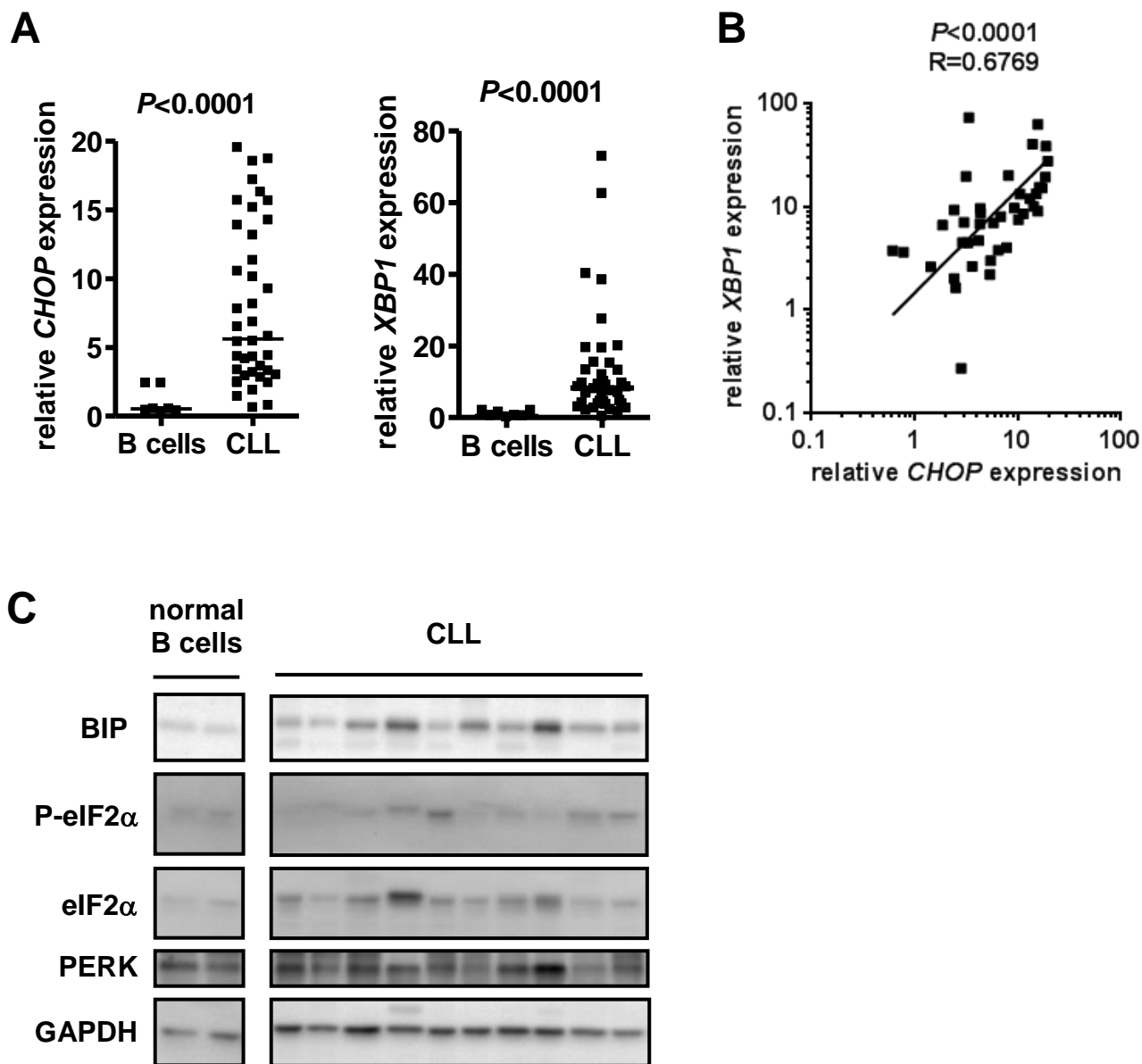


Figure 2

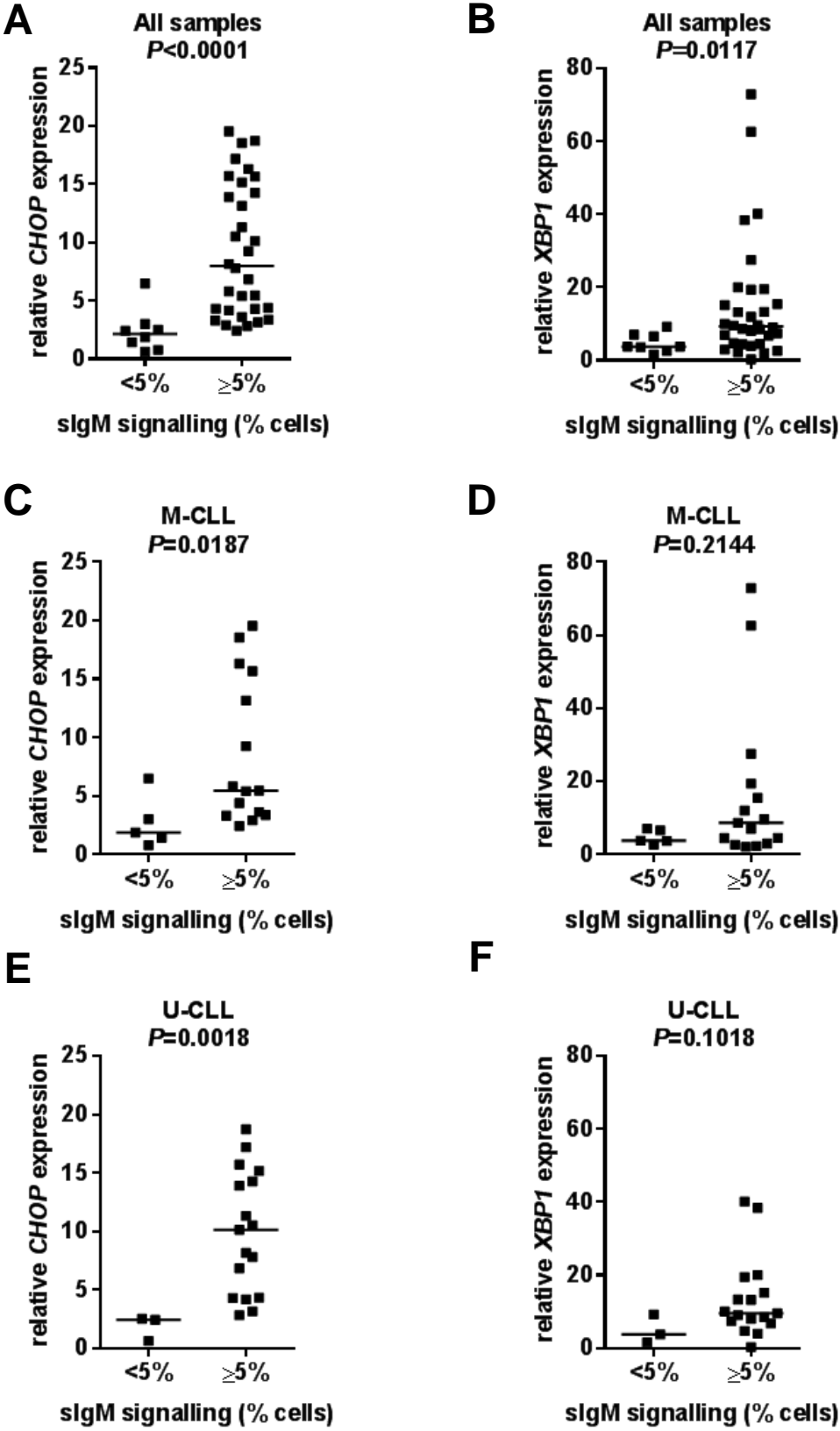


Figure 3

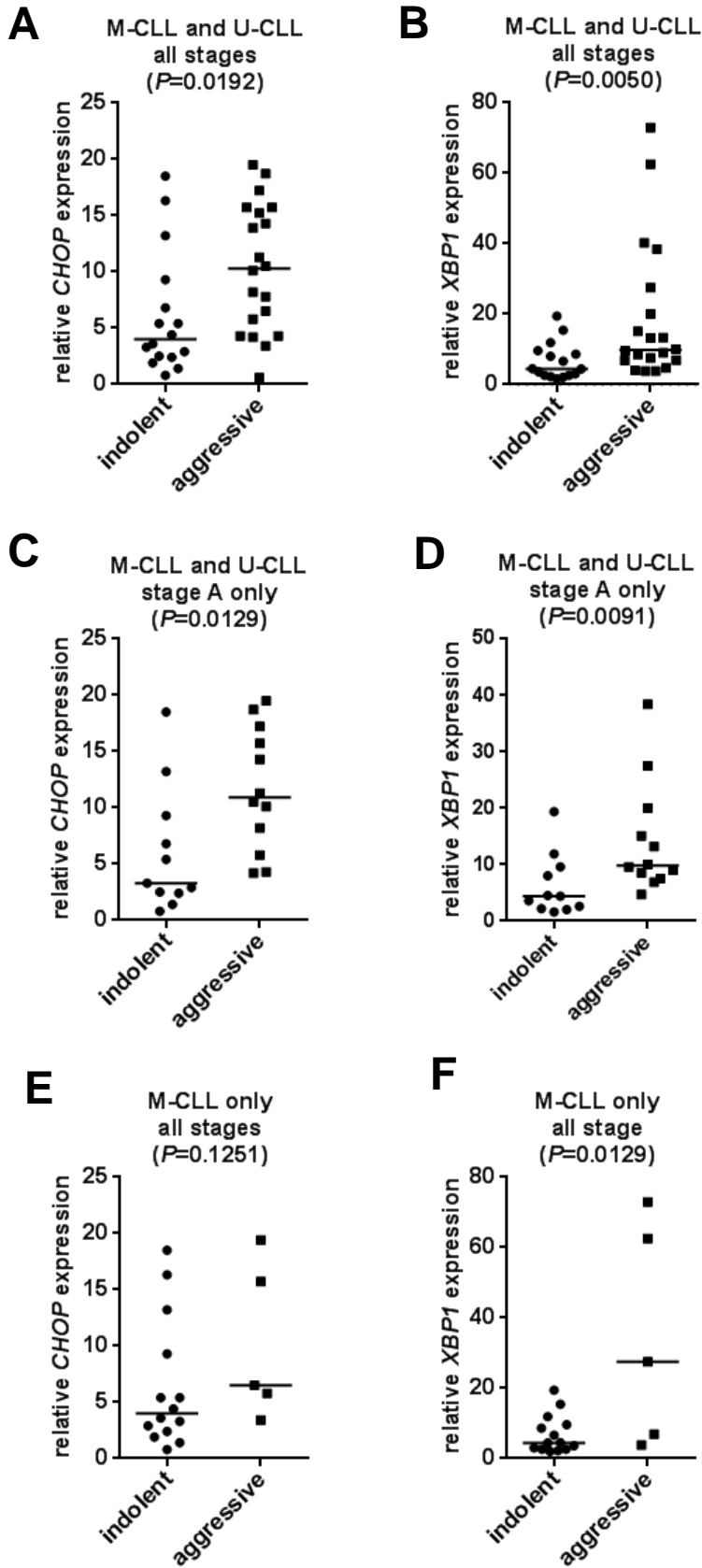
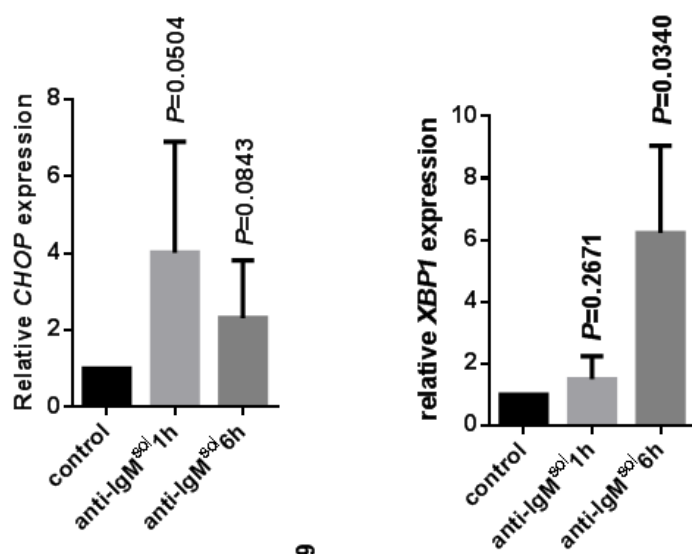
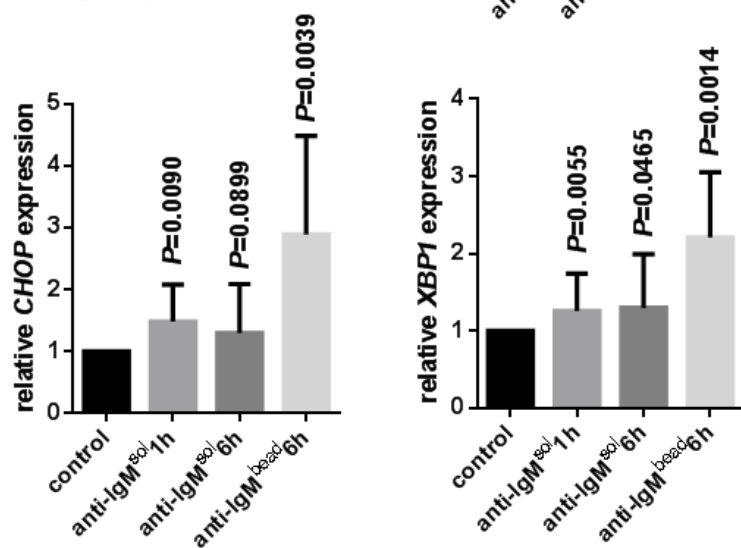


Figure 4

**A**



**B**



**C**

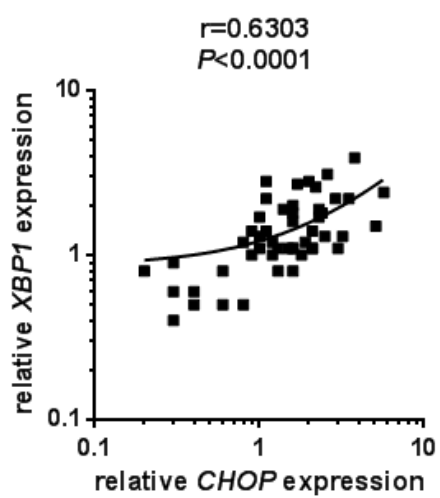


Figure 5

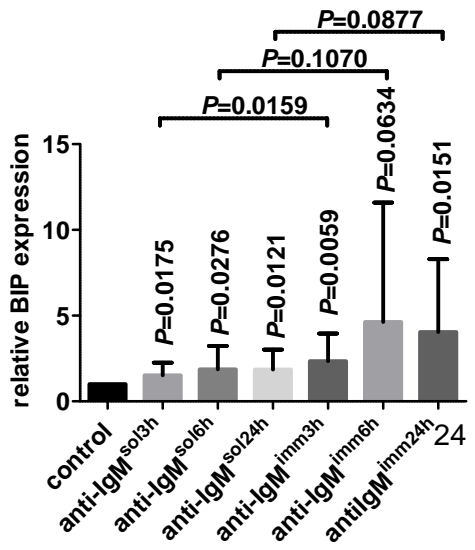
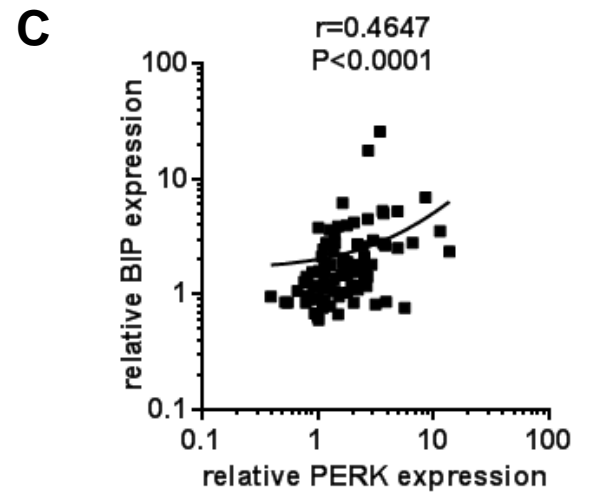
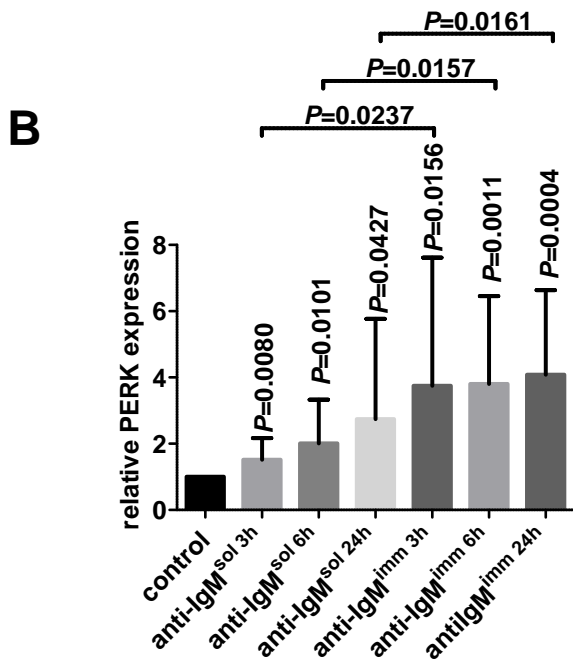
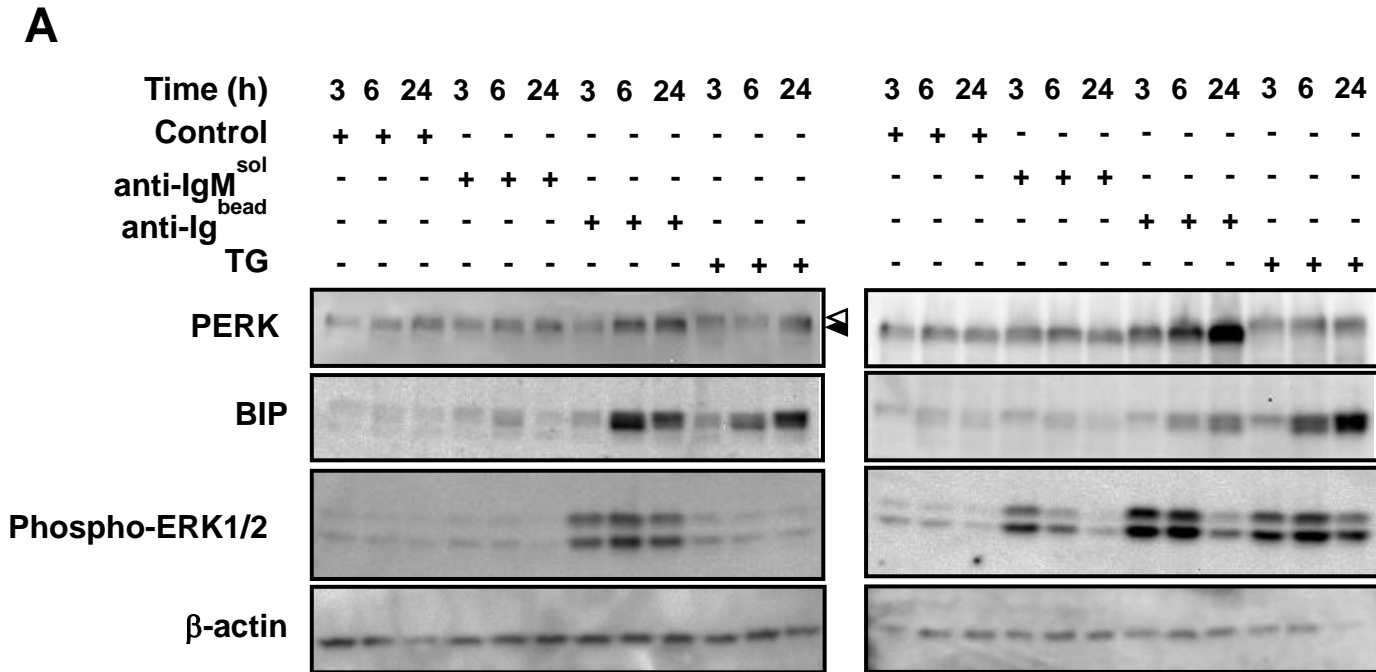




Figure 6

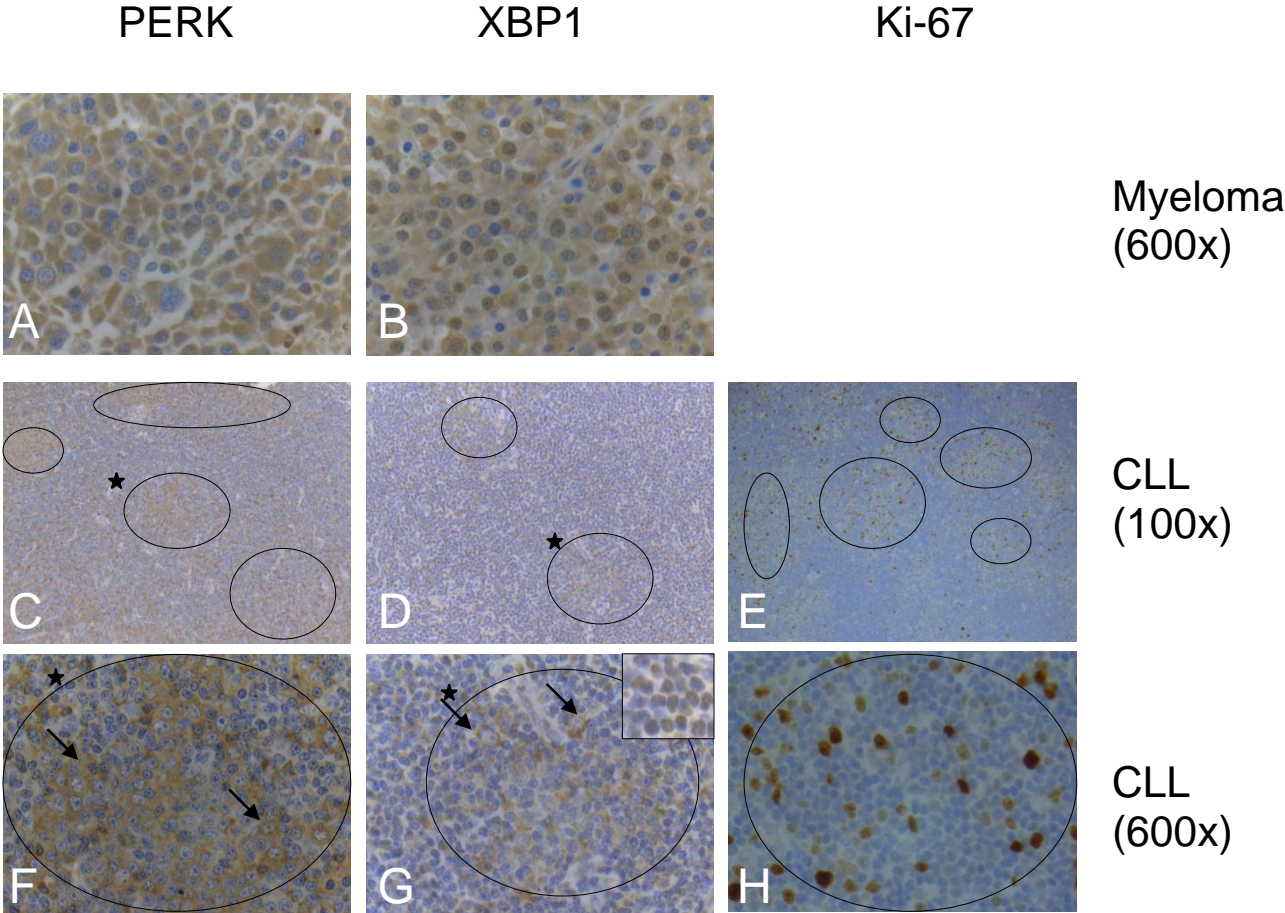
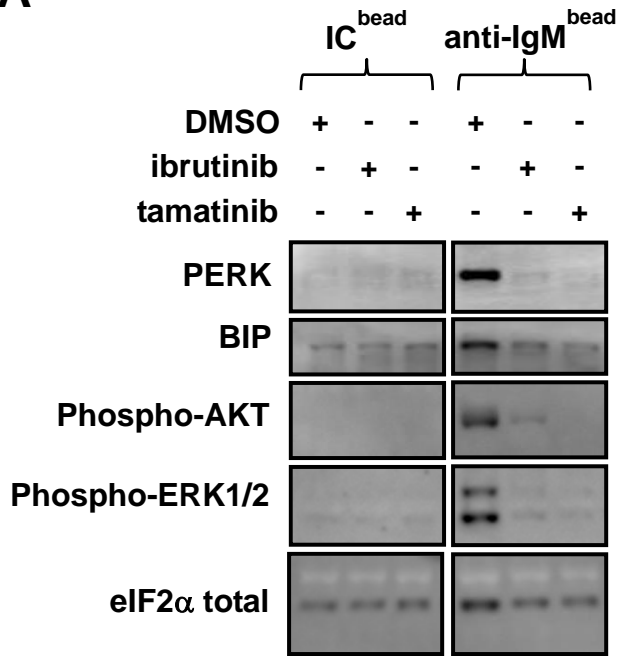
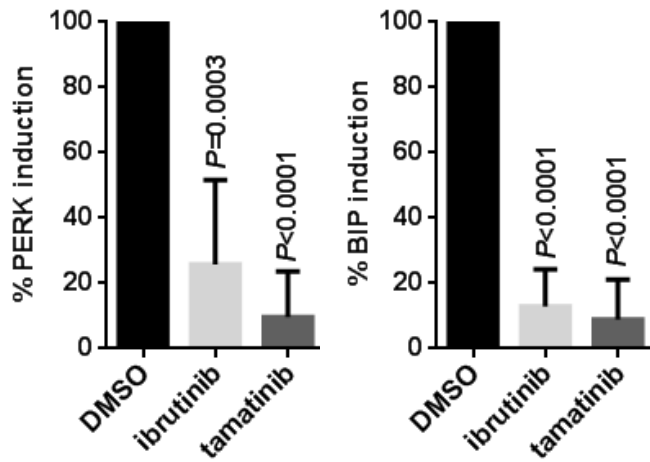


Figure 7

**A**



**B**



# **SUPPLEMENTARY MATERIAL**

*Krysov et al.*

**Supplementary methods**  
**Supplementary Tables S1 and S2**  
**Supplementary Figures S1 to S9**

## Supplementary methods

### *RNA analysis*

Total RNA was isolated using the RNeasy kit (QIAGEN, Crawley, UK) according to the manufacturer's instructions and converted to cDNA using oligo(dT) primers and M-MLV reverse transcriptase (Promega, Southampton, UK). For analysis of *XBP1S* RNA we used the approach described previously (Bagratuni et al. 2010). For quantitative PCR (Q-PCR), PCR reactions were performed using a 7500 Real Time PCR System and TaqMan Universal PCR Master Mix (Applied BioSystems, Warrington, UK) and the following TaqMan probes: Human *B2M* (beta-2-microglobulin) endogenous control (4333766T), *XBP1* (Hs02856596\_m1), *CHOP* (Hs99999172\_m1). Relative RNA quantities were calculated with the equation  $RQ=2^{-\Delta\Delta CT}$  using *B2M* expression as an internal control and normalized so that the expression in normal B cells, or control CLL cells was set to 1.0. Published gene expression array (GEA) data (accession: GDS4176) (Herishanu et al. 2011) were analyzed using the NCBI Gene Expression Omnibus browser (<http://www.ncbi.nlm.nih.gov/geo/>).

### *Protein analysis*

Immunoblotting was performed using the following antibodies: anti-phospho-ERK1/2 (9101), anti-ERK1/2 (9102), anti-PERK (5683), anti-BIP (3183), anti-phospho-AKT (S473) (4060), anti-AKT (9272), anti-phospho-eIF2 $\alpha$  (S51) (3597), anti-eIF2 $\alpha$  (2103) (all from Cell Signaling Technology, Hitchin, UK), anti-XBP1 (619501; BioLegend, London, UK) and anti- $\beta$ -actin (2066; Sigma-Aldrich, Poole, UK). Secondary horseradish peroxidase-conjugated antibodies were from GE Healthcare (Little Chalfont, UK). Densitometry analysis of immunoblot images was performed using Quantity One software (BioRad). In experiments with longer incubations (>6 hours), cells were treated with the caspase inhibitor zVADfmk (50  $\mu$ M, Calbiochem) to minimize secondary events due to apoptosis.

Immunohistochemical analysis was performed using a tissue-microarray prepared from formalin fixed and paraffin embedded lymph node (LN) tissue sections from 11 cases of CLL/small lymphocytic lymphoma (SLL). Immunostaining was performed on sections after deparaffinisation and citrate buffer (pH 6.0) antigen retrieval with anti-XBP1 (ab37152; Abcam), anti-PERK (5683; Cell Signaling Technology) or anti-Ki-67 (MIB1; Dako, Stockport, UK) primary antibodies at a 1:100 dilution. Diaminobenzidine was used for staining development and the sections were counterstained with Mayer's haematoxylin. Multiple myeloma sections were used as a staining positive control.

### *Cell treatments*

For sIgM stimulation, CLL cells were cultured at  $1 \times 10^7$ /ml and treated with 20  $\mu$ g/mL soluble goat F(ab')<sub>2</sub> anti-human IgM (Southern Biotechnology, Cambridge, UK) or goat F(ab')<sub>2</sub> anti-human IgM coated M-280 Dynabeads (Invitrogen, Paisley, UK). The preparation of anti-IgM-coated beads was as described.(Coelho et al. 2013) Cells were treated with antibody-coated beads at a ratio of 2 beads per cell. As controls, cells were treated with soluble or bead-bound, non-immune goat F(ab')<sub>2</sub> (Southern Biotechnology). In experiments using chemical inhibitors, cells were pretreated with ibrutinib or tamatinib (both 10 $\mu$ M; Selleckchem, Newmarket, UK) for 1 hour prior to stimulation with anti-IgM. Thapsigargin and brefeldin A were from Sigma-Aldrich.

### *Statistics*

Statistical analyses were performed using GraphPad Prism 6 software (GraphPad, San Diego, CA, USA).

Bagratuni T, Wu P, Gonzalez de Castro D, et al. XBP1s levels are implicated in the biology and outcome of myeloma mediating different clinical outcomes to thalidomide-based treatments. *Blood*. 2010;116(2):250-253.

Herishanu Y, Perez-Galan P, Liu D, et al. The lymph node microenvironment promotes B-cell receptor signaling, NF-kappaB activation, and tumor proliferation in chronic lymphocytic leukemia. *Blood*. 2011;117(2):563-574.

Table S1

Sample	Stage <sup>a</sup>	anti-IgM-induced Ca <sup>2+</sup> mobilization (max. % responding cells)	<i>IGHV</i> mutation status <sup>b</sup>	ZAP70 <sup>c</sup>	CD38 <sup>c</sup>
154	A	21	U	ND <sup>d</sup>	38
162	C	0	M	39	1
164	A	0	M	1	17
170	A	1	U	26	100
221	A	19	U	16	51
238	A	3	U	82	6
255	C	14	U	25	8
271	A	0	M	31	2
277	A	6	M	0	1
279	B	12	M	0	0
285	A	39	U	35	100
304	B	33	U	24	74
305	C	8	U	65	9
306	A	19	U	23	49
314	A	24	M	1	4
315	A	24	U	15	8
318	C	59	M	2	5
323	A	14	U	67	15
324	A	7	M	1	0
326	B	7	M	8	2
328	A	74	U	16	23
329	A	11	M	0	93
330	A	5	M	66	7
333	A	77	M	1	1
341	NK <sup>d</sup>	39	M	0	80
344	A	40	M	31	60
348	A	19	M	0	4
350	A	6	U	63	95
353	C	73	M	2	39
359	NK	3	U	1	10
361	A	17	U	5	98
383	A	14	U	17	24
385	A	19	U	11	36
391	B	69	M	6	1
392	A	72	M	3	7
393	C	41	U	96	59
394	A	46	U	25	96
399	A	0	M	2	0
401	NK	0	M	21	20
402	A	7	M	14	99
405	A	39	U	57	15
409	B	15	U	77	56
410	NK	25	U	8	56
411	A	61	M	0	99
412	A	65	M	2	98
420	A	63	M	1	100
435	A	37	M	1	29
449	A	5	M	45	11
459	A	43	U	6	44
460	A	49	U	23	30
461	A	5	M	11	4
462	A	11	M	8	3
464	A	21	M	0	3
465	B	7	M	30	11
469	A/B	64	M	2	4
473	A/B	52	U	53	73
474	A	7	U	86	50
475	A	9	M	45	1
476	A	16	U	51	10
482	A	5	M	9	84
489	A	5	M	2	1
500	A	9	U	62	94
505	A	17	U	14	14
518	C	16	M	1	0
520	A	3	U	76	0
524	B	5	M	3	1

<sup>a</sup> Binet stage at diagnosis.

<sup>b</sup> U, unmutated; M, mutated.

<sup>c</sup> % positive cells

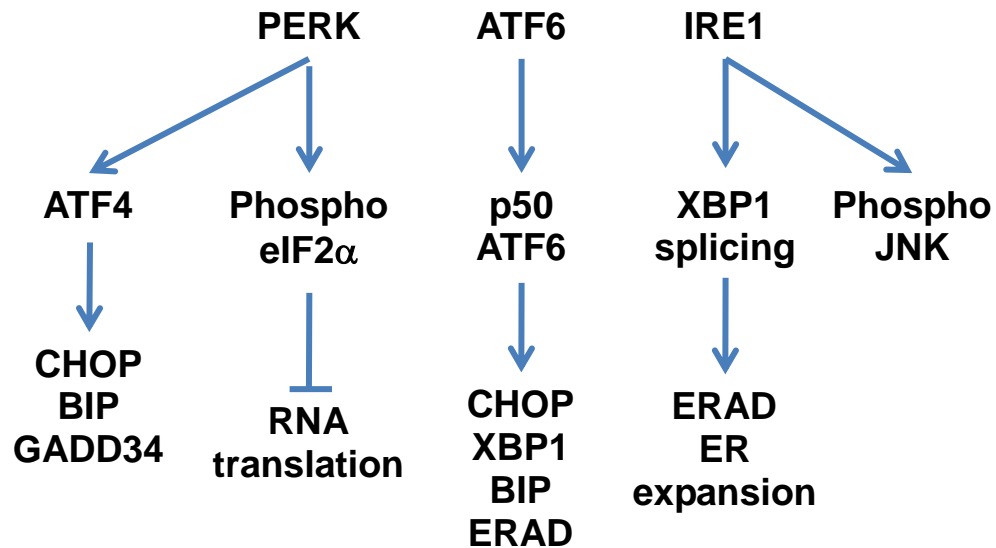
<sup>d</sup> NK, not known; ND, not determined.

Table S2

Sample <sup>a</sup>	XBP1	PERK
1	Nuclear expression in ~10% of small cells outside of proliferation centres	Extranuclear expression in all cells
2	Nuclear expression in ~10% of small cells outside of proliferation centres	Extranuclear expression in all cells
4	Nuclear expression in ~10% of small cells outside of proliferation centres	Extranuclear expression in all cells in PC and 50% of other cells
5	Nuclear expression in ~10% of small cells outside of proliferation centres	Extranuclear expression in all cells
6	Extranuclear expression in occasional blasts in proliferation centres	Extranuclear expression in all cells
7	Nuclear expression in ~10% of small cells. Occasional positive membrane/cytoplasmic expression in proliferation centre blasts	Extranuclear expression in all cells; greater in proliferation centres
8	Extranuclear expression in proliferation centre blasts	Extranuclear expression in all cells; greater in proliferation centres
9	Extranuclear expression in proliferation centre blasts	Extranuclear expression in all cells; greater in proliferation centres
10	Extranuclear expression in proliferation centre blasts; occasional cells with nuclear expression	Extranuclear expression in all cells; greater in proliferation centres
11	Extranuclear expression in proliferation centre blasts	Weak extranuclear expression in proliferation centres only
12	Negative	Extranuclear expression in all cells; greater in proliferation centres
SUMMARY	Infrequent nuclear expression in small cells or extranuclear expression predominantly in proliferation centre blasts	Widely expressed - extranuclear. Often stronger in proliferation centres

<sup>a</sup> Cores for sample 3 were missing from the tissue microarray.

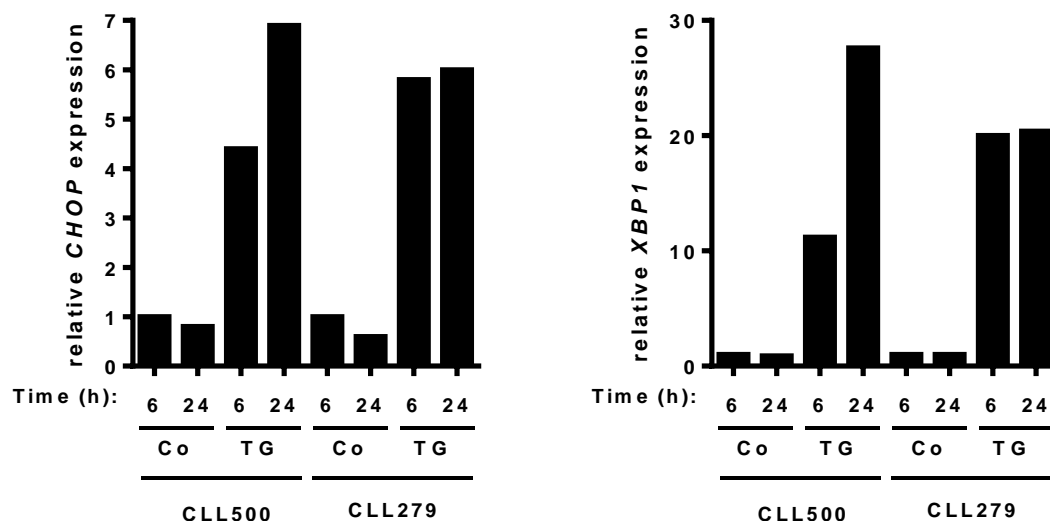
Figure S1



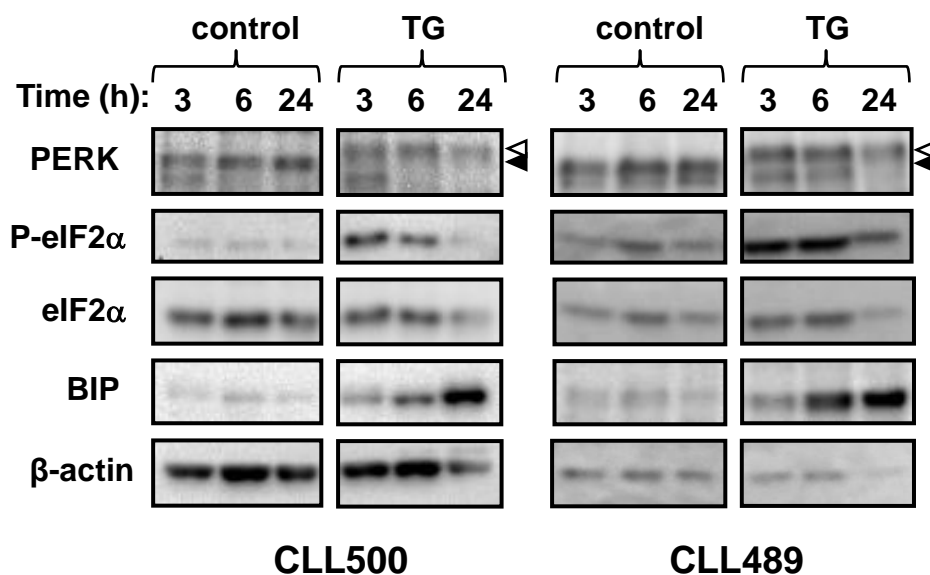
**Overview of UPR pathways.** The UPR is controlled by three endoplasmic reticulum (ER)-resident sensor proteins IRE1, PERK and ATF6. ER stress leads to dissociation of the ER chaperone BIP (GRP78) from these sensors leading to their activation. Full UPR activation is associated with ATF6 transit to the Golgi where it is proteolytically activated. The resultant 50 kDa ATF6 fragment (p50 ATF6) is a nuclear transcription factor that induces expression of UPR-associated genes, including *BIP*, *CHOP* and *XBP1*, and components of the ERAD (endoplasmic reticulum-associated protein degradation) system. IRE1 undergoes autophosphorylation which activates its endoribonuclease activity resulting in a removal of 26-base pair fragment from *XBP1* RNA. The *XBP1* splice variant is translated into XBP1S, a transcription factor which induces expression of chaperones and ERAD proteins. The UPR is a highly flexible response system and variable activation of its downstream effector arms in different cell types or in response to stimuli of differing strength/duration, fine-tunes responses ranging from survival to apoptosis. Prolonged, high-level UPR responses are linked to cell death which is predominantly mediated by JNK1, downstream of IRE1, and, in some cell types, induction of CHOP.



A

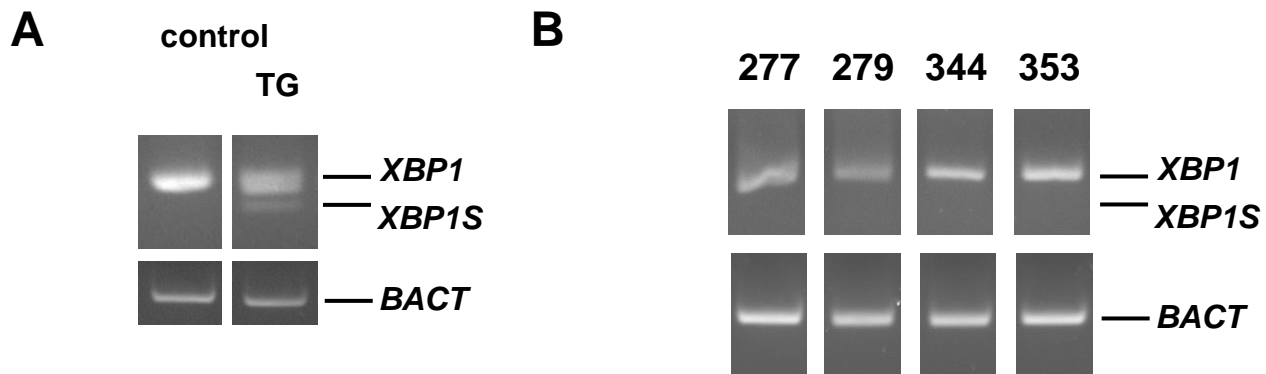


B



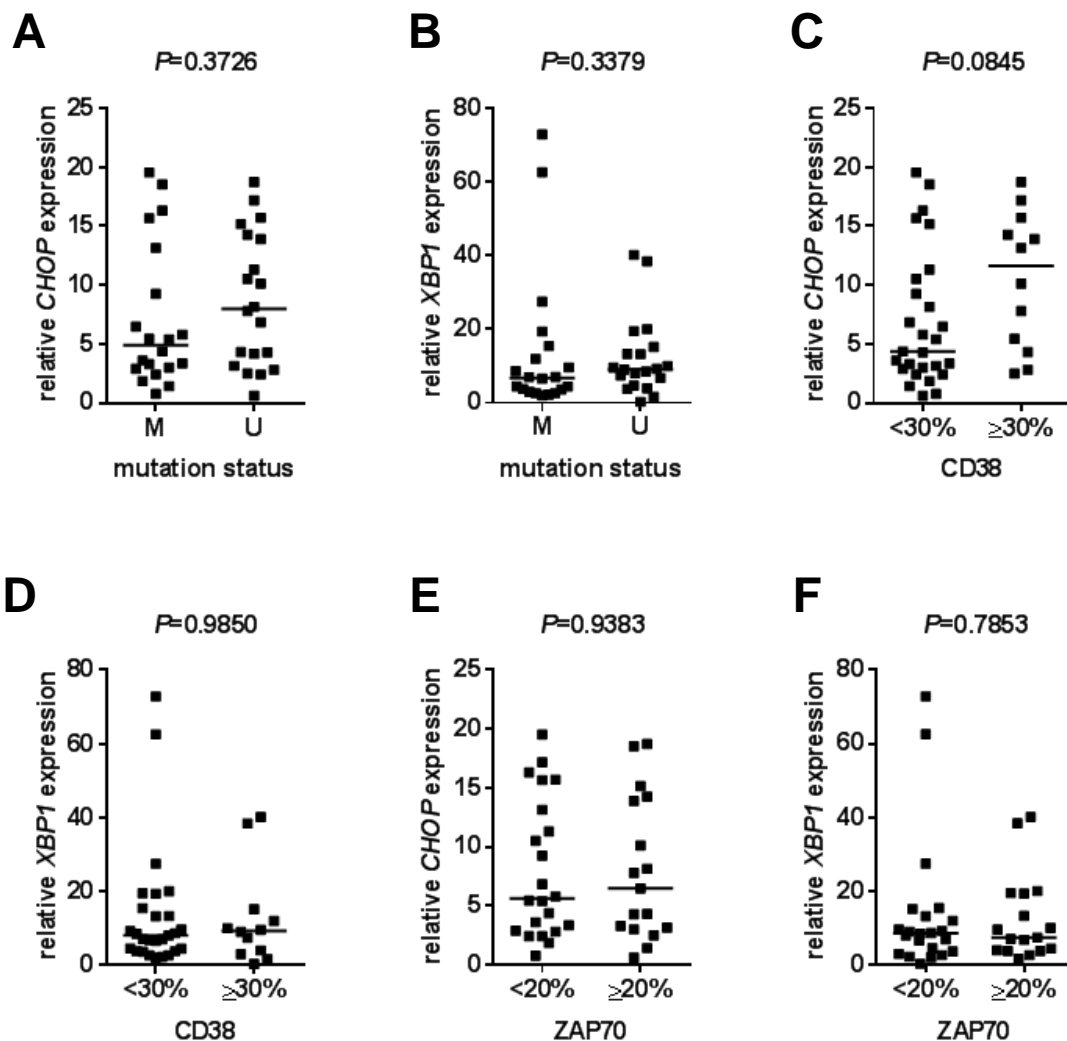
### Regulation of the UPR in thapsigargin-treated CLL cells

CLL cells were treated with thapsigargin (TG; 15 $\mu$ M) or left untreated as a control (Co). Cells were collected after 3, 6 or 24 hours. (A) Q-PCR analysis of *CHOP* and *XBP1* RNA expression. (B) Immunoblot analysis of PERK, total eIF2 $\alpha$ , phosphorylated eIF2 $\alpha$ , BIP and  $\beta$ -actin (loading control). Phosphorylated and non-phosphorylated forms of PERK are indicated by white and black triangles, respectively. For (A), *CHOP/XBP1* RNA expression values were normalised to *B2M* expression and normalised expression values of control cells at 6 hours were set to 1.0. For (B), cells were incubated throughout the experiment in the presence of zVADfmk (50mM) to suppress apoptosis. Data shown were obtained using two samples and are representative of results obtained with 15 samples.



***XBP1S* RNA expression in untreated and thapsigargin-treated CLL cells**

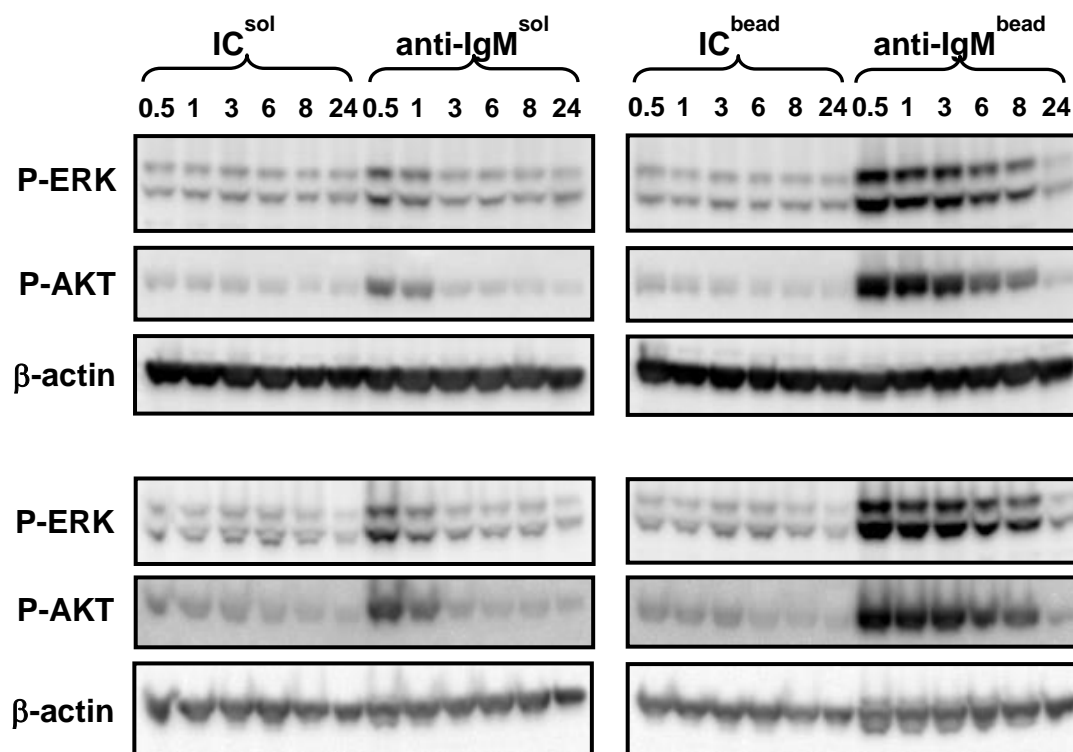
Analysis of full length and spliced *XBP1* RNA in CLL cells using RT-PCR. *BACT* RNA expression is shown as a control. (A) Representative CLL sample treated with thapsigargin (TG; 15 $\mu$ M). (B) Untreated CLL samples. Data shown are representative of results obtained with 30 different samples.



**Correlations between *CHOP* and *XBP1* RNA expression and prognostic features of CLL.**

Correlations between basal *CHOP* and *XBP1* RNA expression and (A,B) *IGHV* mutation status, (C,D) CD38 expression and (E,F) ZAP70 expression in all samples. The statistical significance of differences was analyzed using the Mann-Whitney test.

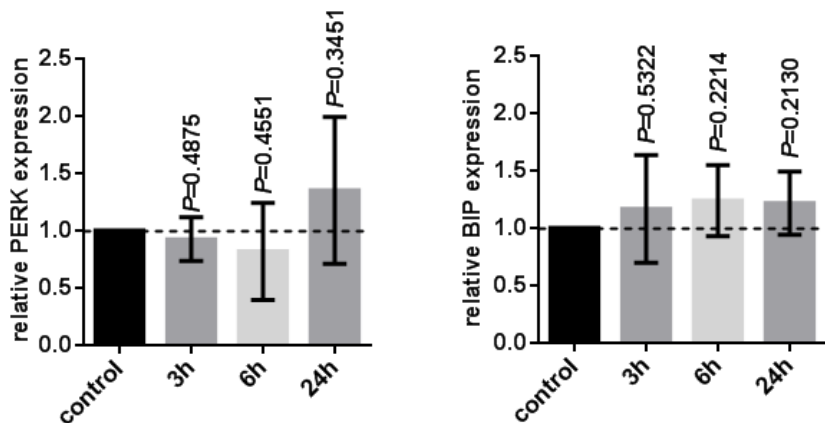
Figure S5



**Effects of soluble or bead-bound anti-IgM on kinase activation**

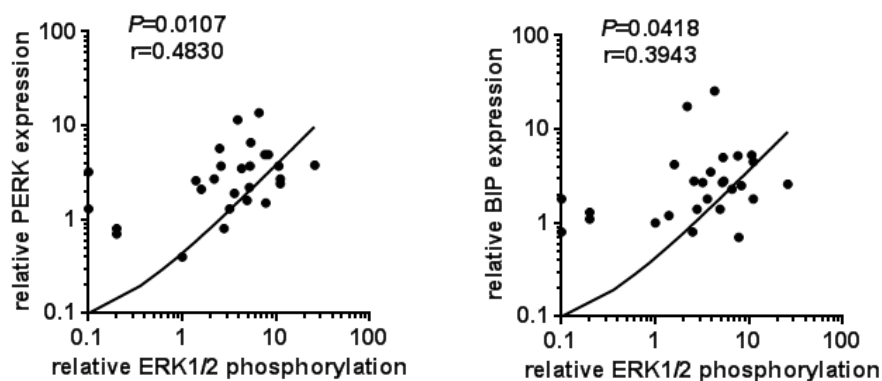
CLL samples were stimulated with soluble (sol) or bead-bound anti-IgM (anti-IgM<sup>bead</sup>) or isotype control (IC) antibodies for up to 24 hours in the presence of zVADfmk. Expression of phosphorylated ERK1/2 (T<sup>202</sup>/Y<sup>204</sup>), phosphorylated AKT (S<sup>473</sup>) and β-actin was analyzed by immunoblotting. Data shown are representative of results obtained with more than 15 samples.

Figure S6



**PERK and BIP expression in control and soluble anti-IgM-treated non-responsive CLL samples.**

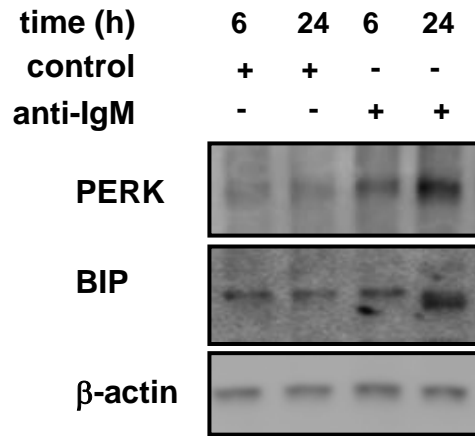
slgM non-responsive CLL samples (n=4) were incubated with soluble anti-IgM for 3, 6 or 24 h and expression of PERK and BIP was analyzed by immunoblotting. Expression values were normalised so that the mean value in control cells at each time point was set to 1.0. Graphs show mean values ( $\pm$ SD). The statistical significance of the differences between control and anti-IgM treated cells are shown for each time point (paired Student's t-test).



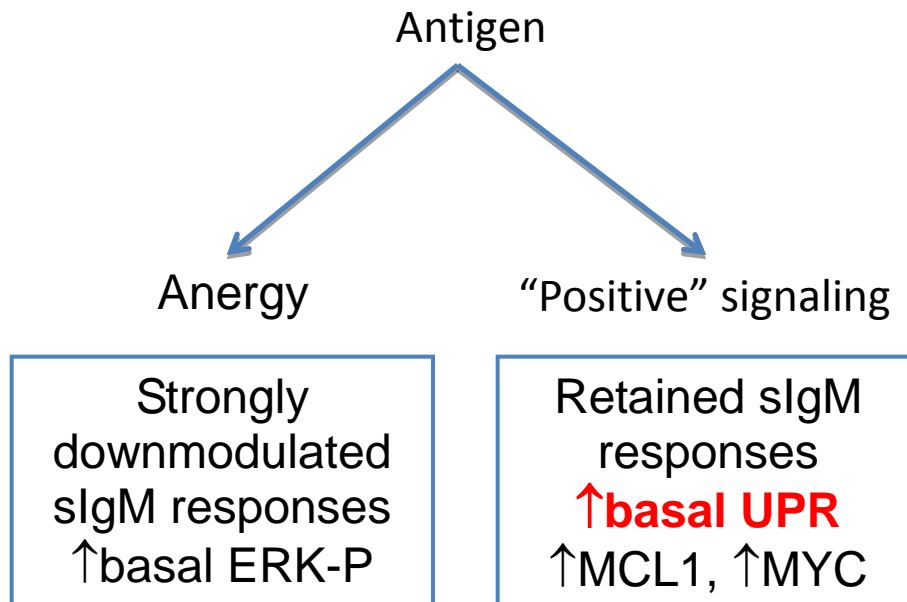
**Comparison of anti-IgM-induced PERK/BIP expression and ERK1/2 phosphorylation in signal responsive samples.**

Parallel immunoblotting was used to quantify PERK, BIP and ERK1/2 phosphorylation for 9 of the samples analyzed in **Figure 5** of the main manuscript. Expression values were normalized to  $\beta$ -actin. We then calculated the expression of each marker in bead-bound-anti-IgM treated cells relative to control cells at the same time point. Graphs include comparisons for data for all time points and show results of linear regression and Spearman correlations.

Figure S8



**PERK and BIP expression in control and anti-IgM-treated normal B cells.** Normal B cells (anti-CD138-depleted) were incubated with soluble anti-IgM or isotype control antibody for 6 or 24 h and expression of PERK, BIP and  $\beta$ -actin (loading control) was analyzed by immunoblotting. Results are representative of two independent preparations of cells.



**A model linking differential antigen signaling via sIgM to modulation of the UPR.**

Antigen signaling results in two predominant signaling responses in CLL; anergy linked to a good prognosis and "positive" growth-promoting signaling linked to more aggressive behavior. BCR-induced UPR activation appears to be linked to positive signaling since basal UPR expression is highest in the subset of samples which retain sIgM signaling responsiveness and is further elevated following treatment with anti-IgM *in vitro* in signal responsive samples.